LBL-19235 c.2

Lawrence Berkeley Laboratory

UNIVERSITY OF CALIFORNIA

Materials & Molecular Research Division

DOCUMENTS SECTION

Presented at the 3rd International
Al-Li Conference, Oxford, England,
July 9-11, 1985

A THEORETICAL ANALYSIS OF THE AGING RESPONSE OF Al-Li ALLOYS STRENGTHENED BY Al_3Li PRECIPITATES

J. Glazer, T.S. Edgecumbe and J.W. Morris, Jr.

June 1985

TWO-WEEK LOAN COPY
This is a Library Circulating Copy
which may be borrowed for two weeks.

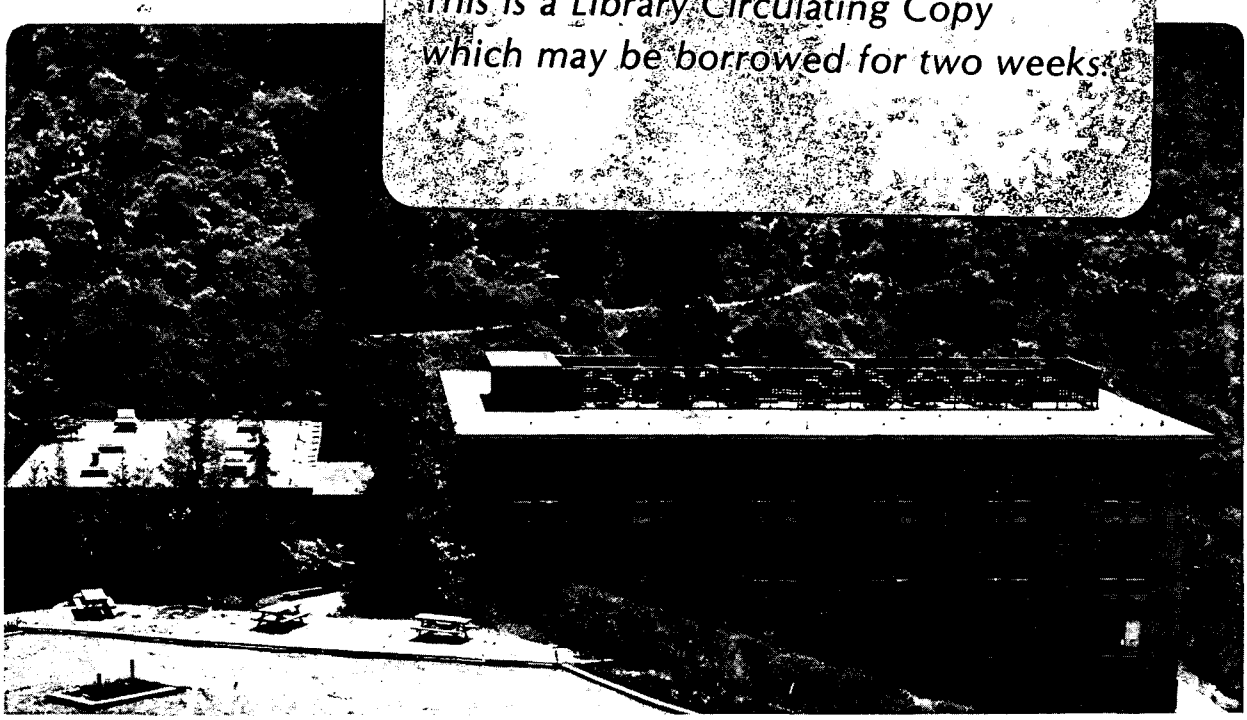

LBL-19235 c.2

Prepared for the U.S. Department of Energy under Contract DE-AC03-76SF00098

DISCLAIMER

This document was prepared as an account of work sponsored by the United States Government. While this document is believed to contain correct information, neither the United States Government nor any agency thereof, nor the Regents of the University of California, nor any of their employees, makes any warranty, express or implied, or assumes any legal responsibility for the accuracy, completeness, or usefulness of any information, apparatus, product, or process disclosed, or represents that its use would not infringe privately owned rights. Reference herein to any specific commercial product, process, or service by its trade name, trademark, manufacturer, or otherwise, does not necessarily constitute or imply its endorsement, recommendation, or favoring by the United States Government or any agency thereof, or the Regents of the University of California. The views and opinions of authors expressed herein do not necessarily state or reflect those of the United States Government or any agency thereof or the Regents of the University of California.

A THEORETICAL ANALYSIS OF THE AGING RESPONSE OF AL-LI ALLOYS STRENGTHENED BY AL_3LI PRECIPITATES

J. Glazer, T.S. Edgecumbe and J.W. Morris, Jr.

Materials and Molecular Research Division
Lawrence Berkeley Laboratory
and
Department of Materials Science and Mineral Engineering,
University of California, Berkeley, CA 94720

ABSTRACT

The possibility of increasing the strength of aluminum-lithium alloys hardened principally by the δ' precipitates was investigated. The elastic theory of phase transformations was used to determine that the δ' precipitate is not expected to deviate from spherical morphology even at very large sizes. The theory of the critical resolved shear stress for dislocation glide through a random array of obstacles was used to predict a moderate strengthening increment if the precipitate size distribution could be made more uniform. Experimental and theoretical hardening curves for an experimentally determined precipitate size distribution were also compared.

I. INTRODUCTION

Although the aluminum-lithium alloys nearing commercialization are strengthened by copper-rich phases, the ideal aluminum-lithium alloy should be primarily strengthened by lithium-rich phases such as Al_3Li, which do not increase the density of the alloy. We have therefore conducted a theoretical investigation of the possibility of achieving significantly greater strengths than realized to date in near-binary alloys strengthened by δ'.

In the nickel-based superalloys it has been possible to obtain considerable strength increments through modification of the composition of the $L1_2$ precipitate γ' either to increase its misfit or to induce precipitation of the tetragonal phase γ''. Both of these avenues have been investigated for aluminum-lithium alloys, but have been unsuccessful thus far. It is possible that the search for elemental additions

with these effects will eventually prove fruitful. In the meantime, near-binary aluminum-lithium alloys will be strengthened primarily by δ' precipitates with relatively low misfit strains.

Given that the crystallography of the δ' precipitate is fixed, we have investigated two other microstructural factors which could have a significant effect on the strength at constant precipitate volume fraction: (1) the precipitate morphology, and (2) the precipitate size distribution. These problems may be examined using the elastic theory of structural transformations and the random array theory of dislocation glide, respectively.

II. MORPHOLOGY

In other alloys hardened by $L1_2$ precipitates, three precipitate morphologies are observed: spherical, cuboidal, and plate-like [1]. Since platelet precipitates provide the greatest strengthening for a given amount of precipitated solute, it would be desirable to induce this morphology. We have focussed initially on identifying the conditions under which each of the observed shapes is preferred.

The linear elastic model of phase transformations is based on the recognition that elastic strains often influence the thermodynamics and kinetics of transformation. The theory may be used to predict the preferred shapes and habits of coherent inclusions [2,3]. The important assumptions are as follows:

(1) A coherent precipitate will have the shape and habit which minimize its contribution to the Helmholtz free energy of the material.

(2) The portion of the energy change which is a function of morphology is the sum of the surface energy and the elastic energy introduced by the precipitate. The surface energy is assumed to be isotropic.

(3) Since in most cases the unconstrained elastic constants of the precipitate are unknown, they are assumed to be the same as those of the matrix. This is a good assumption if the anisotropies are similar.

(4) The elastic energy of a misfitting coherent precipitate has been derived by Khatchaturyan using a version of the Eshelby cycle. The solution is the integral over the precipitate volume

$$\Delta F_{el} = (1/2)\int B(\mathbf{e}) \; |\theta(k)|^2 \; d^3k/(2\pi)^3 \qquad (1)$$

where $B(\mathbf{e})$ is an energy factor which depends on the habit of the precipitate, the elastic constants of the precipitate and the matrix, and the unconstrained transformation strain, and $\theta(k)$ is an amplitude which depends only on the shape of the inclusion. The determination of the preferred shape and habit of the precipitate is accomplished through a minimization of this integral.

(5) The above expression for the elastic energy is easily derived if the transformation is modelled using the Eshelby cycle [2,3,4]. In

the first step, a body the size and shape of the inclusion is cut out of the material and allowed to transform while unconstrained by the matrix. The strain with respect to its original dimensions is designated ε^0, the stress-free transformation strain. Tractions are then imposed on the inclusion to return it to its original size and shape. The energy associated with this step is given by the product of the strain ε^0 with the stress σ^0 required to reverse the transformation strain integrated over the volume of the precipitate

$$\Delta F_1 = \int 1/2\sigma^0_{ij}\varepsilon^0_{ij}\, dV \tag{2}$$

If the inclusion is now allowed to relax into another shape, its energy will decrease by an amount given by the integral over the precipitate volume

$$\int_V (\int_\varepsilon \sigma_{ij} d\varepsilon_{ij}) dV \tag{3}$$

where the ε_{ij} are the elements of the relaxation strain tensor. If the stress in (3) is decomposed into σ^0 and a relaxation stress, equations (2) and (3) may be combined into an expression for the elastic energy

$$\Delta F = \int (1/2\sigma^0_{ij}\varepsilon^0_{ij}\theta(r) - \sigma^0_{ij}\varepsilon_{ij}\theta(r) + 1/2\lambda_{ijkl}\varepsilon^0_{ij}\varepsilon^0_{kl})dv \tag{4}$$

where the integral is now over the total volume of the system , $\theta(\mathbf{r})$ is the particle shape function, which is 1 inside the inclusion and zero outside it, and the λ_{ijkl} are the elastic constants of the precipitate and matrix.

The only unknown parameter in equation (4) is the relaxation strain field. Since the inclusion is a macroscopic defect, this strain field may be determined in the long-wavelength approximation by requiring that it obey static equilibrium. The Fourier transform of the strain must then be

$$\varepsilon_{ij}(\mathbf{k}) = \Omega_{im}(\mathbf{e})\sigma^0_{ml}e_j e_l \theta(\mathbf{k}) \tag{5}$$

where $\Omega(\mathbf{e})=(k)^2 A^{-1}_{ij}(\mathbf{k})$, A_{ij} is the dynamical matrix of the elastic medium and $\mathbf{e}$ is a unit vector in the direction of $\mathbf{k}$. Substituting into (4) gives the equation (1) for ΔF where $B(\mathbf{e})$

$$B(\mathbf{e}) = \lambda_{ijkl}\varepsilon^0_{ij}\varepsilon^0_{kl} - e_i\sigma^0_{ij}\Omega_{jk}(e)\sigma^0_{kl}e_l. \tag{6}$$

The function $B(\mathbf{e})$ is a scalar energy factor which depends on particle shape only through the direction of the $\mathbf{k}$-vectors. $B(\mathbf{e})$ is positive semi-definite so that the lattice is mechanically stable.

The shape factor $\theta(\mathbf{k})$ is the Fourier transform of the real space shape function $\theta(r)$. Its amplitude depends on the inclusion shape through the allowed values of $\mathbf{k}$.

It can be shown easily that an infinitely thin plate is always the elastically preferred morphology of the precipitate. If the function $B(\mathbf{e})$ depends on $\mathbf{e}$, then there is some value of $\mathbf{e}$ for which $B(\mathbf{e})$ has its

minimum value B(**n**). The lower bound for the elastic energy is then given by

$$\Delta F \geq 1/2B(\mathbf{n})\int|\theta(\mathbf{k})|^2 d^3k/(2\pi)^3 = (V/2)B(\mathbf{n}) \tag{8}$$

where V is the volume of the precipitate. The energy is minimized when the shape factor $\theta(\mathbf{k})$ approaches a δ-function with **k** equal to **n**, that is, when the precipitate is an infinitely thin plate with normal vector **n**.

The minimum energy shapes for a cubic inclusion in a anisotropic cubic matrix can be predicted easily in the limits of zero and infinite volume. At small volumes, the precipitate will be spherical because the surface energy term will dominate. At large sizes, the surface-to-volume ratio is low, and the precipitate will be a thin plate with a well-defined habit which minimizes the volumetric elastic energy term.

The regimes in which these morphologies are stable may be determined by comparing their energies. The sphere to plate transition may be modelled by considering the energy of an ellipsoid as a function of aspect ratio. Figures 1-3 illustrate the variation with aspect ratio of the surface, elastic, and total energies as a function of the precipitate volume. (The aspect ratio, K, is defined so that a sphere has an aspect ratio of one and plates and rods have aspect ratio which are greater than, and less than one respectively. The parameter g is a dimensionless variable given by $(\gamma/c_{44}(\varepsilon^o)^2)(4\pi/3V)^{1/3}$ where γ is the surface energy per unit area). Figure 4 compares these energies with the energy of the cube shape, which was computed separately. From these plots we have obtained the following results:

(1) The sphere is stable at small sizes and the thin plate at very large sizes as expected. The cube is stable in an intermediate range.

(2) The sizes above which the cube and plate are preferred were calculated for δ' in aluminum, and γ' in nickel. A surface energy of 10 erg/cm^2 was assumed in all calculations. The numerical results (given in Table 1) predict that spherical and cuboidal γ' should be stable in nickel-based superalloys, as observed, but that cuboidal δ' would not be stable until the precipitate had a mean diameter of more than 60 meters!

(3) The size at which the sphere is no longer preferred is a strong function of the anisotropy ratio of the matrix. Since aluminum is nearly isotropic the spherical shape remains stable to very large sizes; the elastic energy is not significantly lowered by the shape change.

(4) Other results indicate that a sphere is never the stable shape of a tetragonal precipitate in a cubic matrix.

This model can be used to examine a number of other relevant problems such as the effect of external stress on the precipitate morphology, the morphology of a tetragonal precipitate in a cubic matrix, and the influence of precipitate-precipitate interactions on precipitate morphology.

III. PRECIPITATE SIZE DISTRIBUTION

Given that the δ' precipitates are likely to be spherical under all conditions, we have also investigated the potential yield strength increment obtainable in aluminum-lithium alloys by optimizing the precipitate size distribution. We have approached this problem by calculating the critical resolved shear stress (CRSS) for the glide of a dislocation through a random array of point obstacles.

The random array solution for the CRSS for dislocation glide is based on a simple idealization of the general problem [5,6]. It has been used with reasonable sucess to model a number of experimental situations [7,8,9]. The chief assumptions are as follows:

(1) The dislocation is a flexible line of constant line tension T for a given mean square obstacle spacing l_s.

(2) The obstacles to dislocation glide are modelled as a random array of immobile point barriers. The properties of the point obstacle are adjusted so that the interaction of the dislocation with the obstacle is mathematically equivalent to its interaction in the glide plane with the physical obstacle.

(3) The configuration of the dislocation is described by a unique set of pinning points. The CRSS of the array is reached when the dislocation bypasses the weakest point in the strongest configuration.

(4) For a random array of identical obstacles the problem may be solved analytically using standard statistical techniques. It is convenient to define a dimensionless CRSS

$$\tau^* = \tau l_s b/2T \tag{9}$$

where b is the Burgers' vector in the glide plane. The analytic solution is then given by

$$\tau^* = 0.8871(\beta)^{3/2} \tag{10}$$

where β is a dimensionless obstacle strength given by

$$\beta = F/2T \tag{11}$$

and F is the force to bypass the obstacle.

(5) The CRSS for a mixture of obstacle types is a quadratic sum

$$\tau^2 = \Sigma\, x_\alpha(\tau_\alpha)^2 \tag{12}$$

where x_α is the fraction of obstacles of type α and τ_α is the CRSS for an array containing obstacles of type α only. Computer simulation indicates that the quadratic sum is a good approximation if the distribution of obstacle sizes is relatively continuous [10].

In order to study the effect of the δ' precipitate size distribution (PSD) on the yield strength of the alloy the following addi-

tional assumptions were made:

(1) The precipitates coarsen according to the LSW rate law and at constant volume fraction (in the interior of a grain) [11].

(2) The shape of the PSD as a function of $r/\bar{r}$ does not evolve during coarsening [11].

(3) Each spherical precipitate may be reduced to a set of point obstacles whose strengths correspond to the effective radii of the precipitate in the glide planes it intersects. Therefore, even if all precipitates are the same size, there will be a distribution of obstacle sizes in the glide plane.

(4) The strength of the obstacles is assumed to be a function of the radius of the sheared ordered precipitate only. This is equivalent to neglecting the misfit of the precipitate.

(5) The strengths of the obstacle may be related to the maximum obstacle strength which correponds to the looping radius, at which Orowan looping is first preferred over shearing of the precipitate. The Orowan condition puts an upper limit on the strength of the obstacle whatever its physical size. Based on available TEM micrographs, an upper limit on the looping radius in aluminum-lithium is approximately 300Å for a mean square particle spacing of about 1.1μm [12]. The antiphase boundary energy is not required to compute the obstacle strengths.

(6) There is considerable confusion in the literature over the appropriate form of the line tension. We have adopted the approach of Bacon, Kocks, and Scattergood [13] and taken the line tension to be

$$T = (Gb^2/4\pi(1-\upsilon))\ln(l_s/b). \tag{13}$$

This is the correct form of the line tension for screw dislocations. It is not necessary to consider edge dislocations since macroscopic yielding requires the motion of screw, edge, and mixed dislocations and it is harder to move screw dislocations through the array.

We have also adopted the upper limit on β of 0.7 suggested by Bacon, Kocks, and Scattergood.

(7) The calculated CRSS due to the obstacle distribution represents the increment in the total strength of the alloy due to precipitate hardening only and should properly be denoted $\Delta\tau$.

These criteria allow the CRSS for hardening by δ' to be calculated for various PSD's. We have calculated the CRSS for experimentally obtained PSD's measured by Gu et al. [11] and Baumann [14], respectively, and for the case of uniform precipitate size. The PSD's and the corresponding 'aging curves' are shown in Figures 5 and 6 respectively. As can be seen from the figures, the more sharply peaked the distribution, the more effectively it strengthens. This result is in qualitative agreement with the results of a study by Munjal and Ardell [15] of the effect of PSD's on the CRSS of Ni-Al alloys. The theoretical increment in $\Delta\tau_c$ in Figure 6 is approximately 30%, so this result may have

alloy design implications.

A direct comparison of the theoretical and experimental strengthening increment from the coarsening of δ′ is possible for the PSD from Gu et al. [11] for Al-2.78Li-0.3Mn aged at 200°C which is shown in Figure 5. The experimental and theoretical aging curves are shown in Figure 7. The theoretical coarsening rate has been fixed using the experimentally determined LSW rate constant. Since the quenched alloy undoubtedly contains some atom clusters, the theoretical aging curve has been shifted to slightly shorter times to obtain the best fit. The strength increment for the both yield strength curves has been taken as the strength above the lowest measured strength. To convert the theoretical CRSS values to yield strengths, a Taylor factor of 3 has been assumed. The figure shows that the theoretical and experimental aging curves are in excellent agreement up to peak strength. Beyond peak strength, the model is no longer valid since it does not account for the uncoupling of the paired dislocations after Orowan looping begins. This uncoupling would cause the strength to drop off more gradually after peak strength. The theoretical aging curve for a uniform distribution of precipitates is shown for comparison.

In the future, we hope to extend this model to consider the effect of other strengthening precipitates such as thin plates and to other problems such as the prediction of texture and the superposition of several hardening mechanisms.

ACKNOWLEDGEMENTS

The authors are grateful to Drs. T.H. Sanders, Jr. and S.F. Baumann for helpful discussions, experimental data, and access to unpublished work. This work was supported by the Director, Office of Basic Energy Sciences, Materials Science Division of the U.S. Department of Energy under Contract No. DE-AC03-76SF00098. One of the authors, JG, was supported by an ATT Bell Laboratories Fellowship.

REFERENCES

1. H. Gleiter and E. Hornbogen, Mat. Sci. Eng., **2**, 1967, 285.

2. A.G. Khachaturyan, **Theory of Structural Transformations in Solids**, Wiley and Sons, New York, 1983.

3. J.W. Morris, Jr., A.G. Khachaturyan and S.H. Wen, in **Solid-Solid Phase Transformations**, H.I. Aaronson, D.E. Laughlin, R.F. Sekerka and C.M. Wayman, eds., The Metallurgical Society-AIME, Warrendale, PA, 1983, p.101.

4. S.H. Wen, E. Kostlan, M. Hong, A.G. Khachaturyan, and J.W. Morris, Jr., Acta Met., **29**, 1981, 1247.

5. K. Hanson and J.W. Morris, Jr., J. Appl. Phys., **46**, 1975, 983 and 2378.

6. J.W. Morris, Jr. and D.H. Klahn, J. Appl. Phys., **45**, 1974, 2027.

7. A. Melander, Scand. J. Metall., **7**, 1978, 109.

8. A. Melander and P.Å. Persson, Acta Met., **26**, 1978, 267.

9. A. Melander and P.Å. Persson, Metal Science, **12**, 1978, 391.

10. S. Altintas, PhD. thesis, University of California, Berkeley, 1978.

11. B.P. Gu, G.L. Liedl, T.H. Sanders, Jr., and K. Welpmann, Mat. Sci. and Eng., in press.

12. J. Th. M. DeHosson, A. Huis in't Veld, H. Tamler and O. Kanert, Acta Met., **32**, 1984, 1205.

13. D.J. Bacon, U.F. Kocks, and R.O. Scattergood, Phil. Mag., **28**, 1973, 1241.

14. S.F. Baumann, unpublished work.

15. V. Munjal and A.J. Ardell, Acta metall., **24**, 1976, 827.

Table I. Numerical results for the minimum characteristic diameter (in μm) of the cube and plate. Experimental data is given where available.

PPT	cube		plate	
	theory	expt	theory	expt
δ'-Al	1.4	>0.3	>60m	-
γ'-Ni	0.13	0.1-0.2	200μm	-

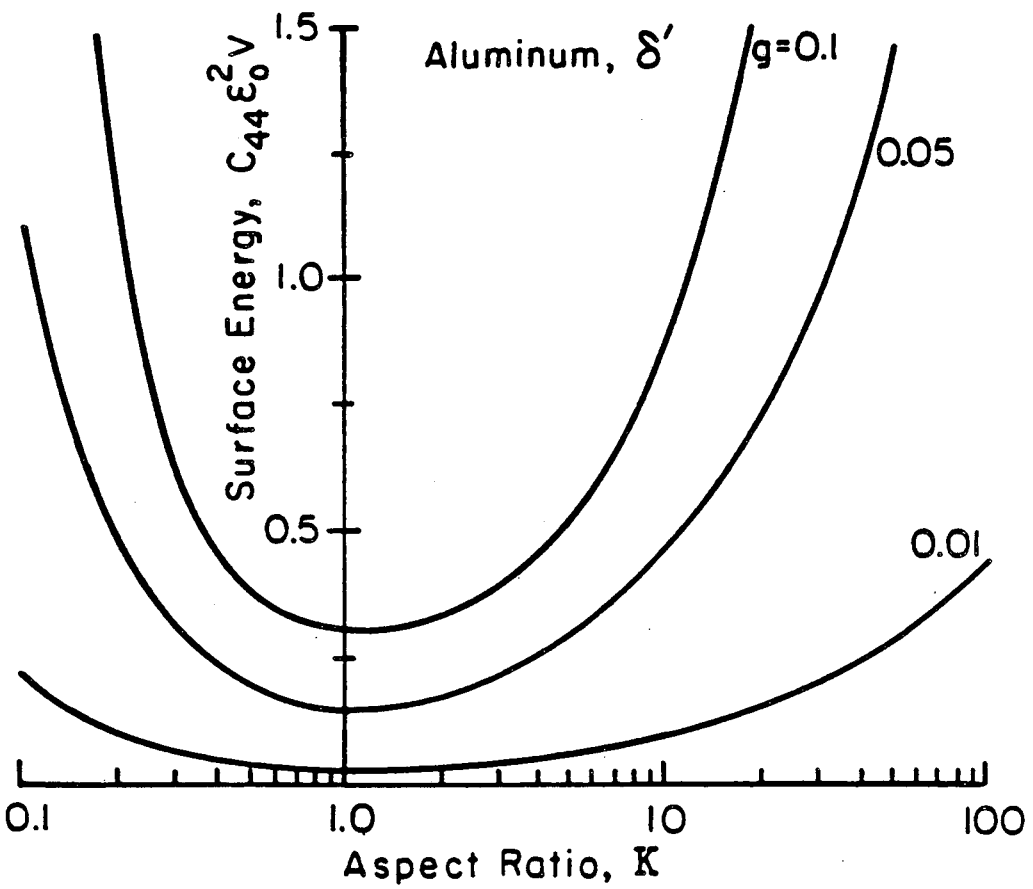

XBL856-6359

1. Surface energy of δ′ precipitate as a function of aspect ratio. The parameter g is given by $(\gamma/c_{44}(\varepsilon^o)^2)(4\pi/3V)^{1/3}$.

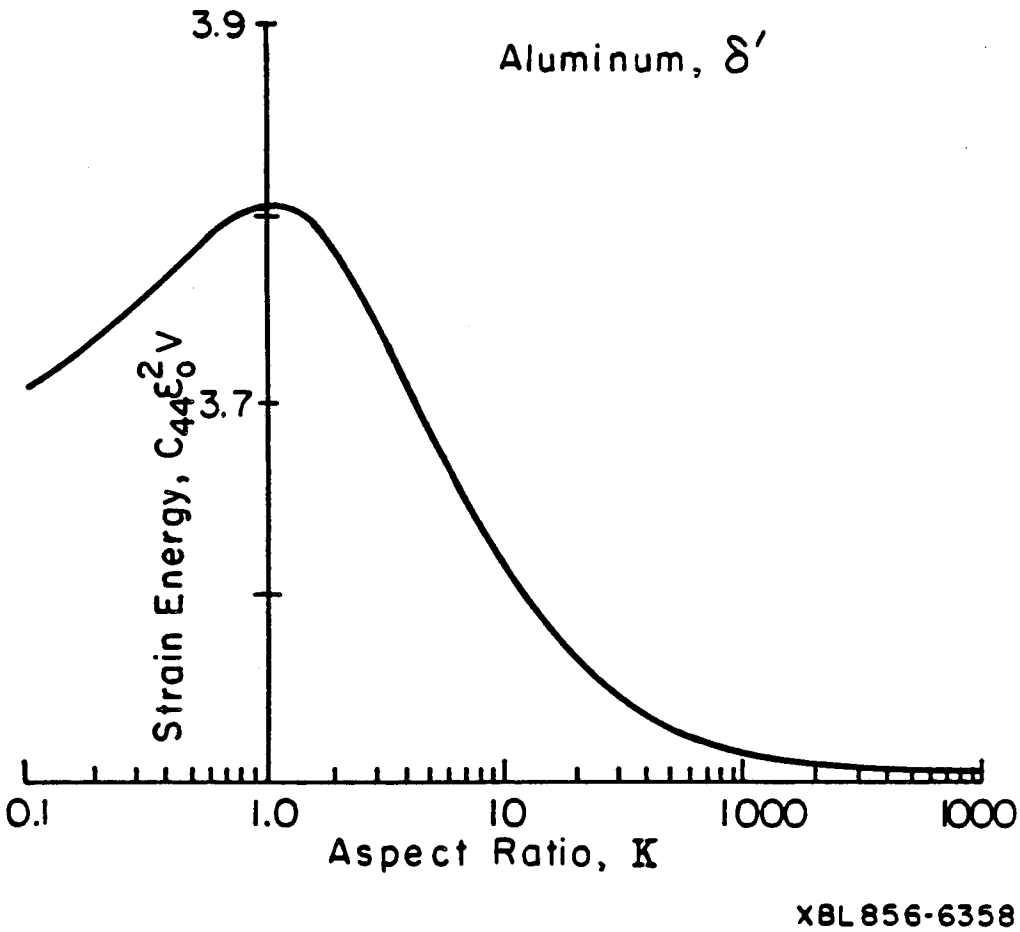

2. Elastic strain energy of the δ′ precipitate as a function of aspect ratio and the parameter g.

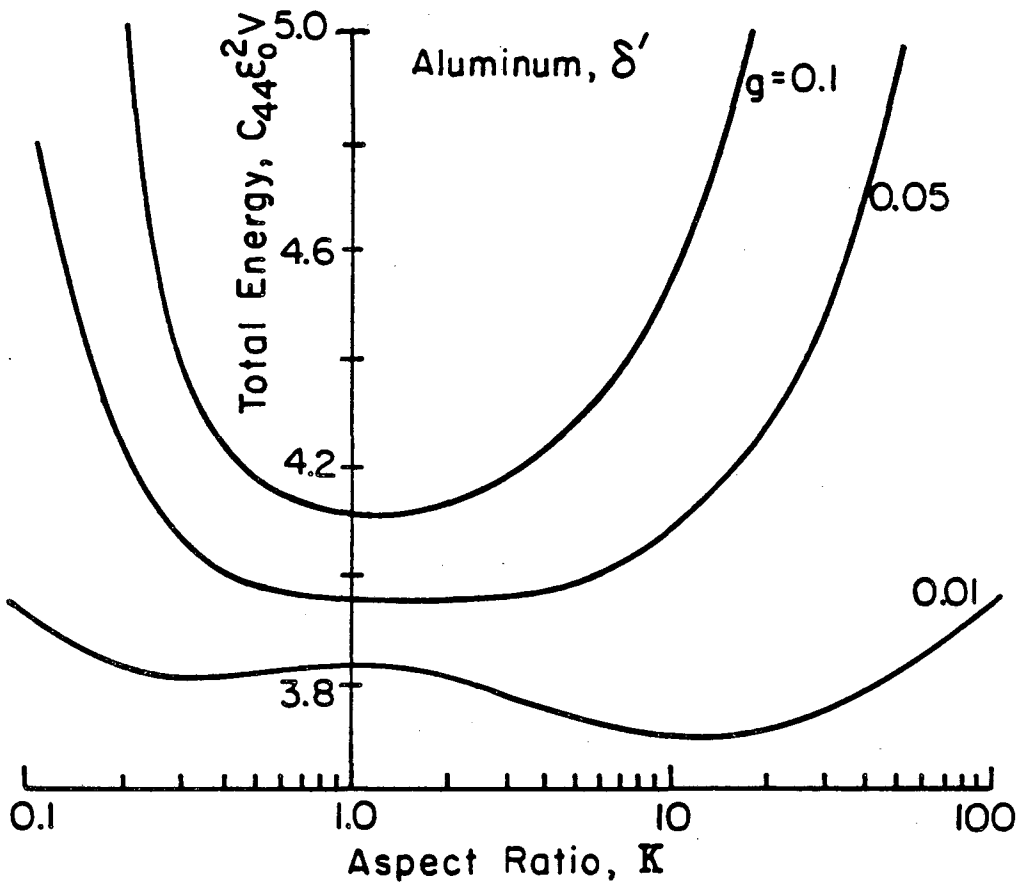

XBL 856-6360

3. Total energy of the δ′ precipitate as a function of aspect ratio and the parameter g.

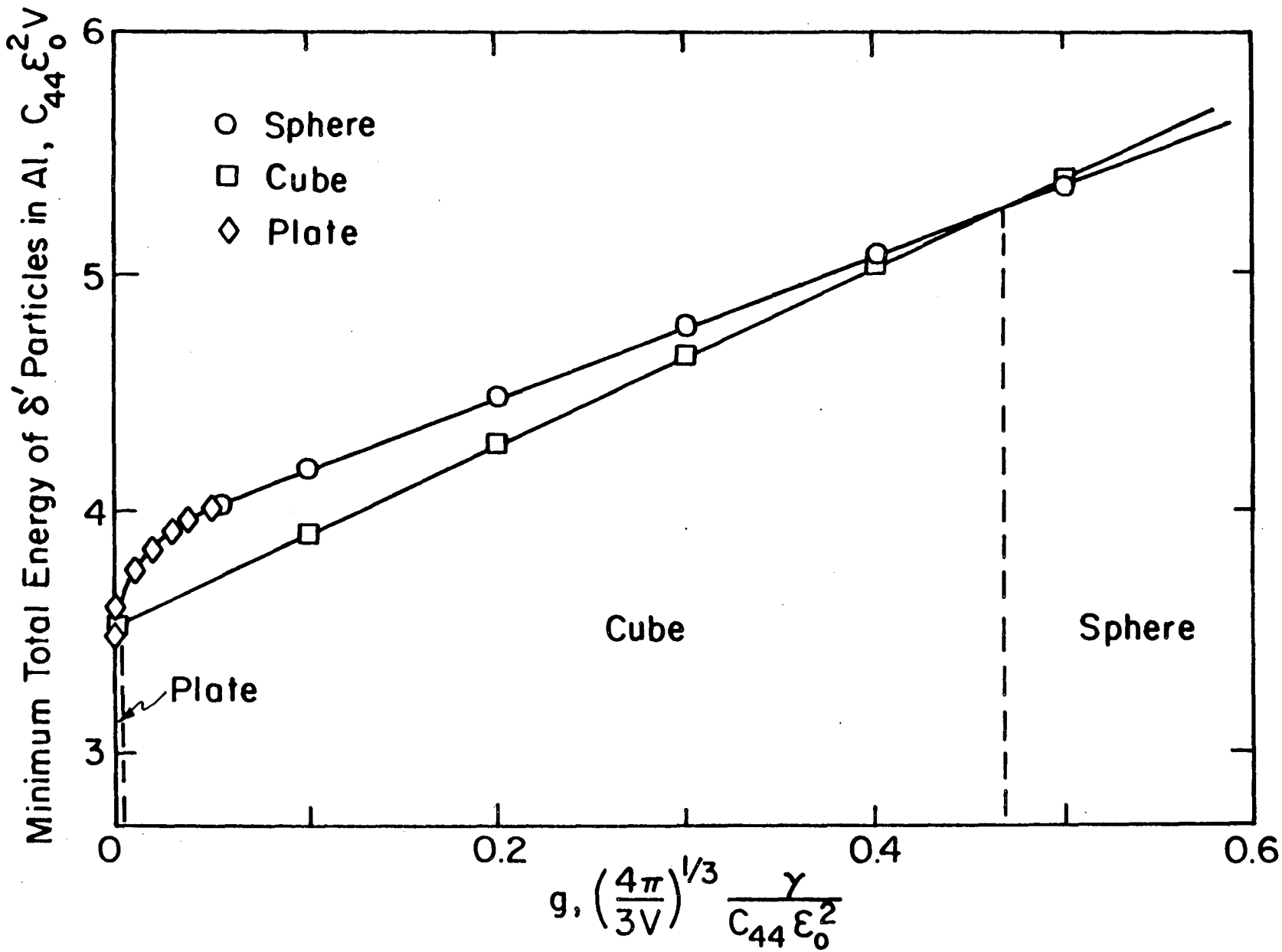

XBL 852-5853

4. Relative energies of the sphere, cube, and plate morphologies as a function of g.

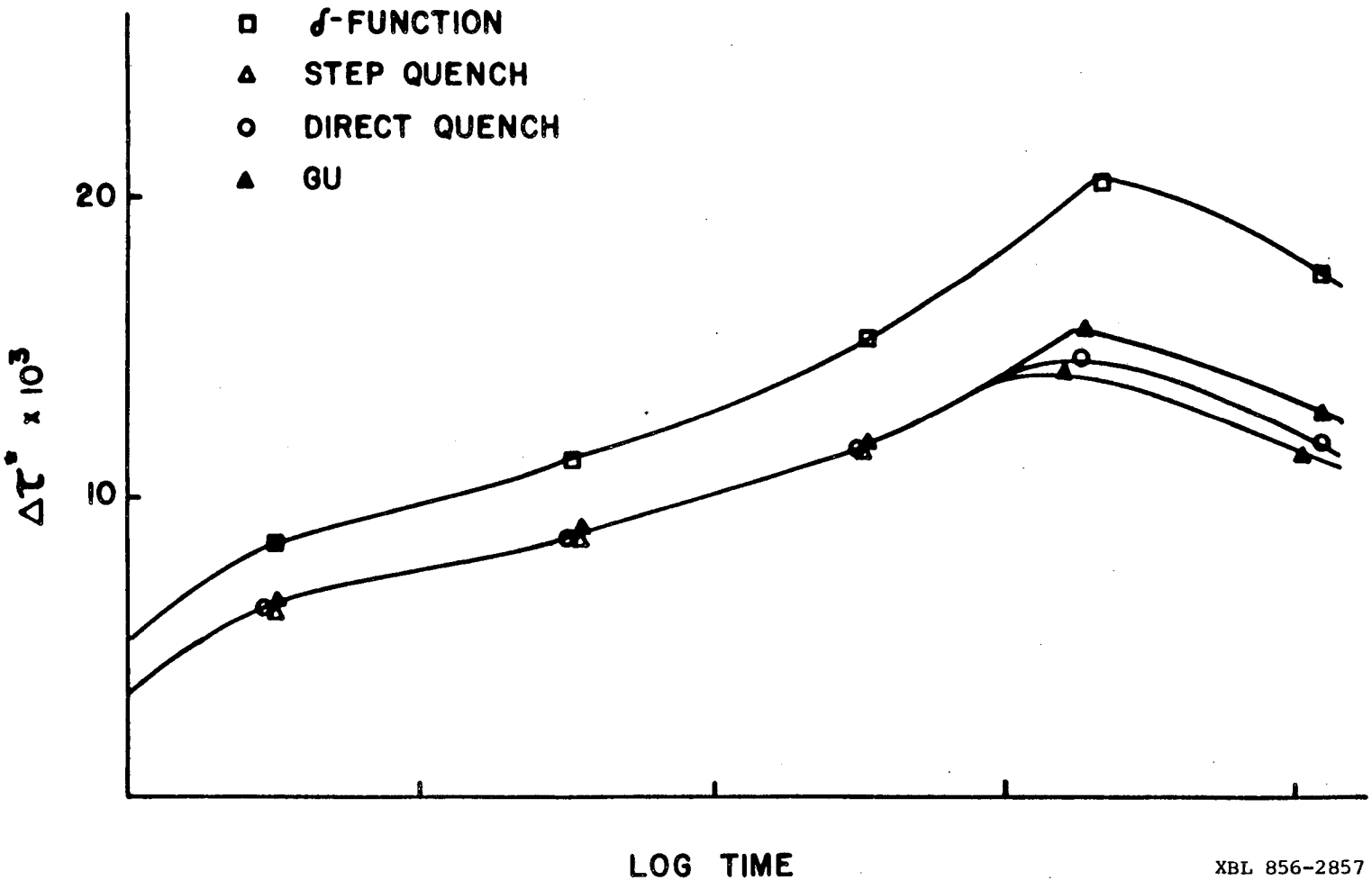

XBL 856-2857

5. Experimentally determined precipitate size distributions for some aluminum-lithium alloys.

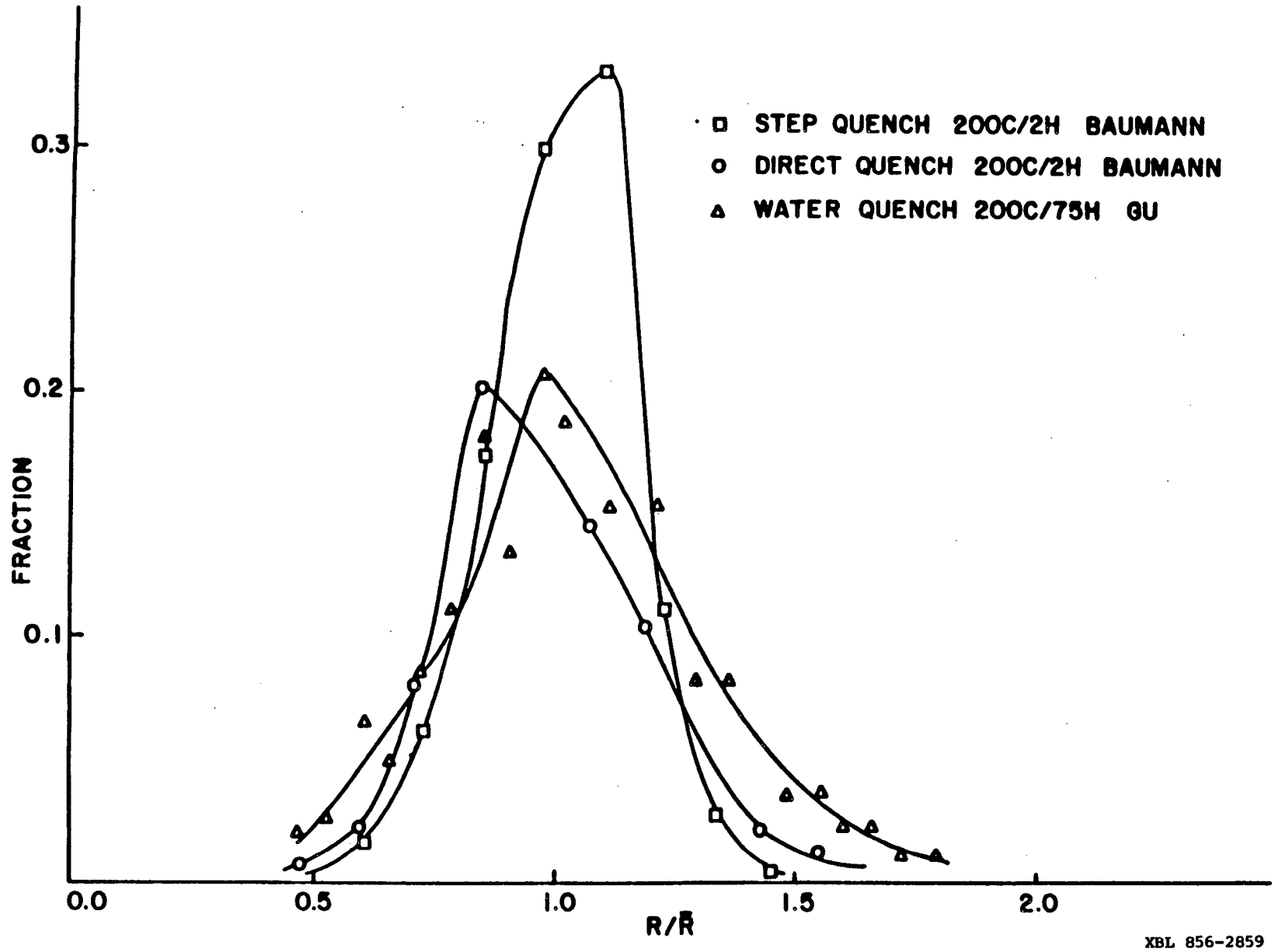

6. Comparison of the variation of the critical resolved shear stress with aging time for the precipitate size distributions in Figure 5.

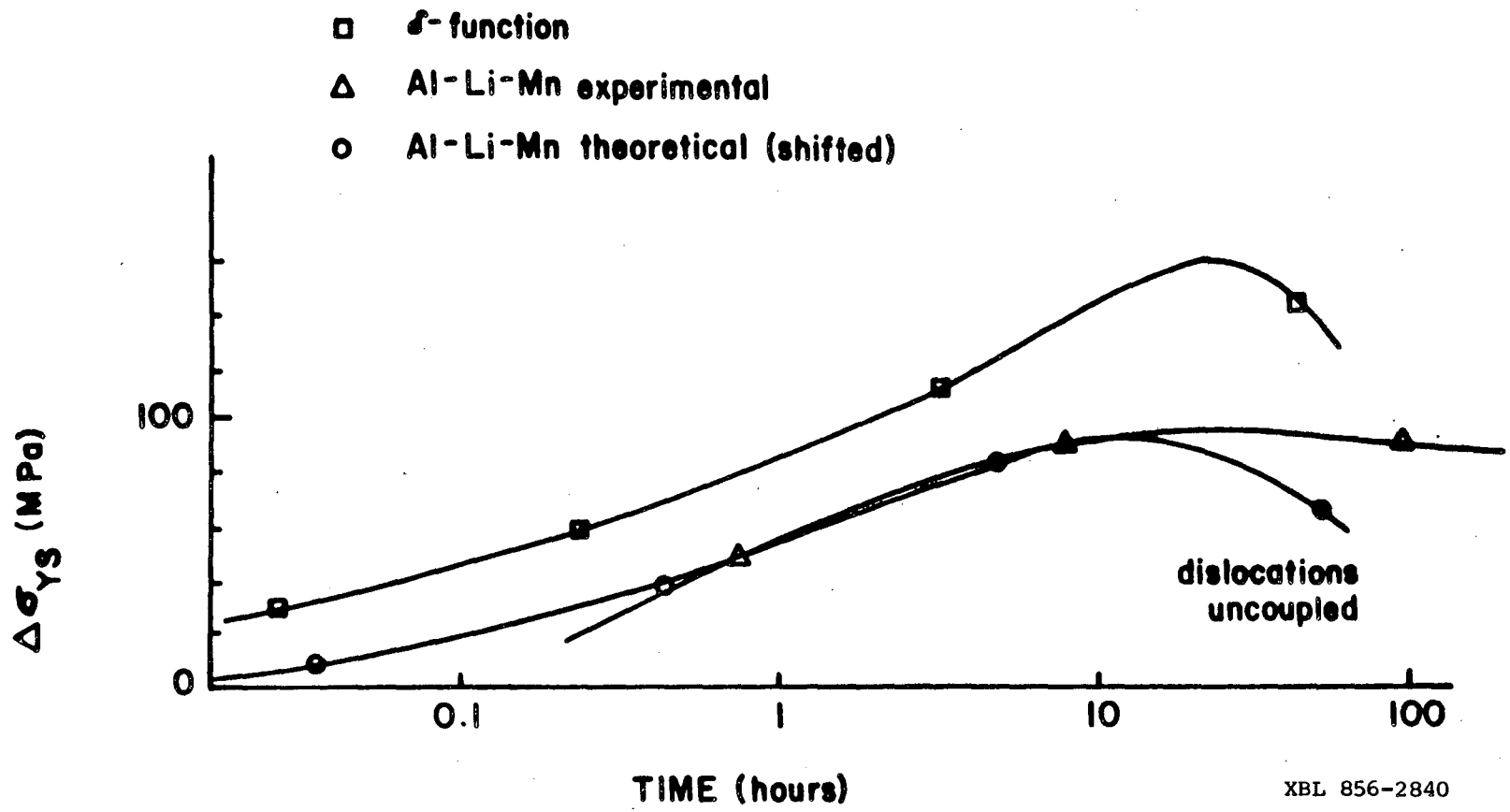

7. Comparison of the theoretical and experimental aging curves for Al-2.78Li-0.3Mn alloy. Time scale refers to experimental curve.

This report was done with support from the Department of Energy. Any conclusions or opinions expressed in this report represent solely those of the author(s) and not necessarily those of The Regents of the University of California, the Lawrence Berkeley Laboratory or the Department of Energy.

Reference to a company or product name does not imply approval or recommendation of the product by the University of California or the U.S. Department of Energy to the exclusion of others that may be suitable.

LAWRENCE BERKELEY LABORATORY
TECHNICAL INFORMATION DEPARTMENT
UNIVERSITY OF CALIFORNIA
BERKELEY, CALIFORNIA 94720